# Effective elastic properties of two dimensional multiplanar hexagonal nanostructures

T. Mukhopadhyay[a], A. Mahata[b], S. Adhikari[a,*], M. Asle Zaeem[b]

[a]*College of Engineering, Swansea University, Swansea, UK*
[b]*Department of Materials Science and Engineering, Missouri University of Science and Technology, Rolla, USA*

## Abstract

A generalized analytical approach is presented to derive closed-form formulae for the elastic moduli of hexagonal multiplanar nano-structures. Hexagonal nano-structural forms are common for various materials. Four different classes of materials (single layer) from a structural point of view are proposed to demonstrate the validity and prospective application of the developed formulae. For example, graphene, an allotrope of carbon, consists of only carbon atoms to form a honeycomb like hexagonal lattice in a single plane, while hexagonal boron nitride (hBN) consists of boron and nitrogen atoms to form the hexagonal lattice in a single plane. Unlike graphene and hBN, there are plenty of other materials with hexagonal nano-structures that have the atoms placed in multiple planes such as stanene (consists of only Sn atoms) and molybdenum disulfide (consists of two different atoms: Mo and S). The physics based high-fidelity analytical model developed in this article are capable of obtaining the elastic properties in a computationally efficient manner for wide range of such materials with hexagonal nano-structures that are broadly classified in four classes from structural viewpoint. Results are provided for materials belonging to all the four classes, wherein a good agreement between the elastic moduli obtained using the proposed formulae and available scientific literature is observed.

*Keywords:* Hexagonal nano-structures; Effective elastic modulus; Analytical closed-form formulae; graphene; hBN; stanene; $MoS_2$

*Corresponding author: S. Adhikari
*Email addresses:* 800712@swansea.ac.uk (T. Mukhopadhyay), akm6w3@mst.edu (A. Mahata), S.Adhikari@swansea.ac.uk (S. Adhikari), zaeem@mst.edu (M. Asle Zaeem)

## 1. Introduction

The fascinating properties of graphene has initiated an enormous interest among the scientific community for exploration of prospective alternative two-dimensional materials that could possess exciting electronic, optical, thermal, chemical and mechanical characteristics [1–3]. The intense research in quasi-two-dimensional materials started with feasible isolation of the single layer carbon atoms [4]. Over the last decade the interest in this quasi-two-dimensional family of materials has expanded from hexagonal boron nitride (hBN), BCN, graphene oxides to Chalcogenides like $MoS_2$, $MoSe_2$ and other two dimensional materials like stanene, silicene, sermanene, phosphorene, borophene etc. [5, 6]. It is however necessary to study these materials at nano-scale as most of the fascinating characteristics are in atomic scale and single layer forms [7]. Among different such materials, as discussed above, hexagonal nano-structure is a very prominent structural form [2]. The common practises to investigate these materials are first principle studies/ ab-initio [8–10], molecular dynamics [11] and molecular mechanics [12], which can reproduce the results of experimental analysis with an expense of economically expensive and time consuming supercomputing facilities. Analytical models leading to closed form formulae are presented by many researchers for materials having hexagonal nano-structures such as graphene [13, 14] and hBN [15]. An informative study is recently reported considering analytical mechanical characterization of different such hexagonal monoplanar structural forms [16]. This approach of mechanical property characterization is computationally very efficient, yet accurate. However, the analytical models for hexagonal nano-structures developed so far are limited to monoplanar structural forms, where all the atoms stay in a single plane. Most of the quasi-two-dimensional materials, as discussed above, posses a structural form where the atoms are found to be placed in multiple planes as shown in figure 1. From the figure it is quite evident that even though the nano-structure has a hexagonal top view, two different atoms (indicated by two different colors) are placed in different planes (three planes can be clearly identified and the top and bottom planes are symmetric with respect to the mid-plane). Thus there is a strong rationale to develop a generalized compact analytical model leading to closed-form and high fidelity expressions for characterizing the mechanical properties of hexagonal multiplanar nano-structures.
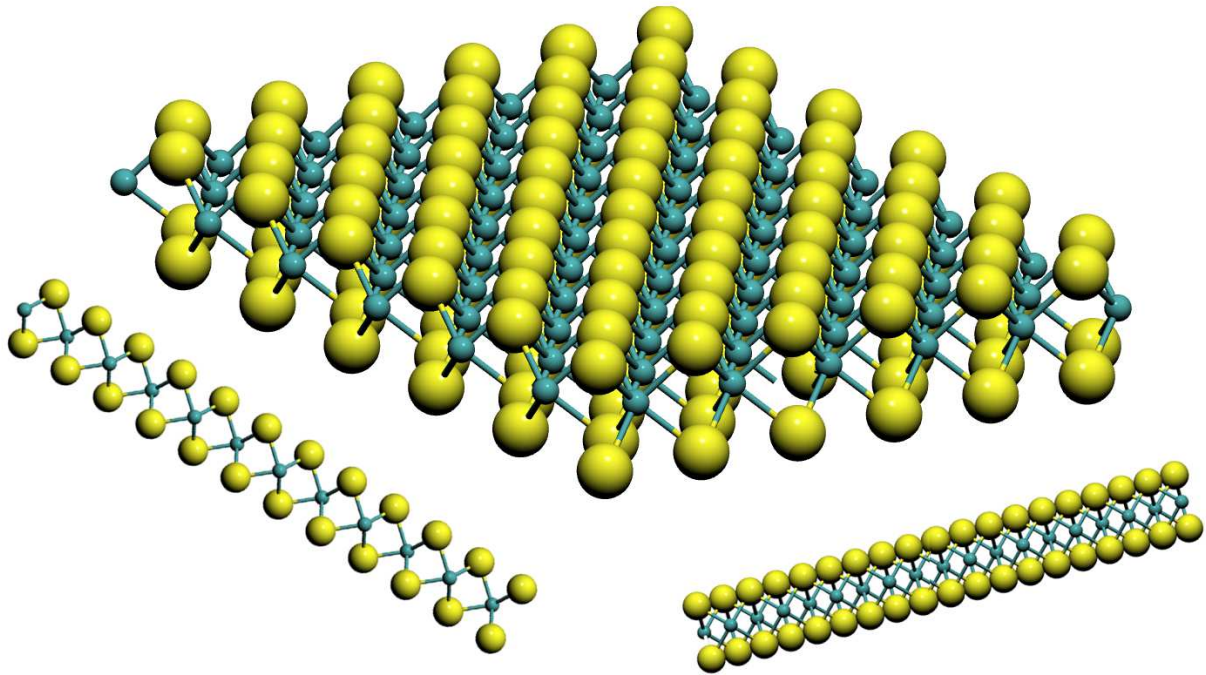
(a)
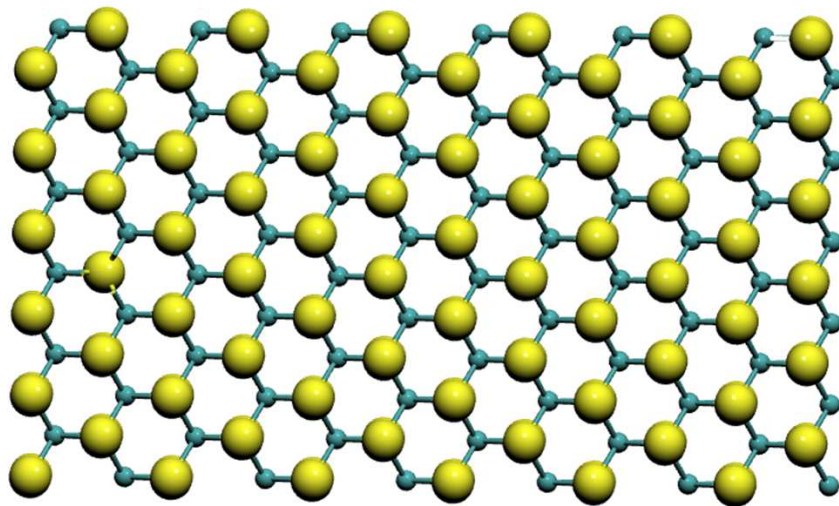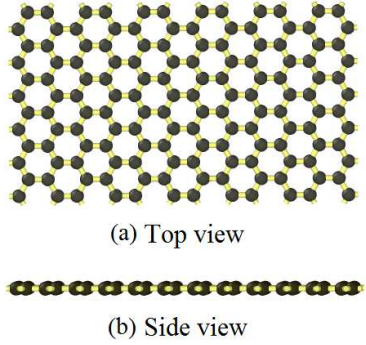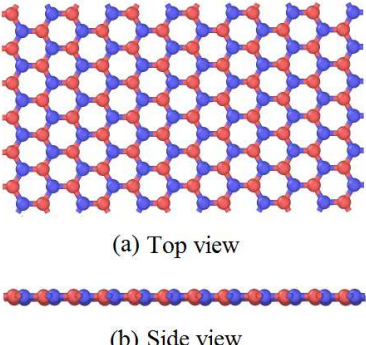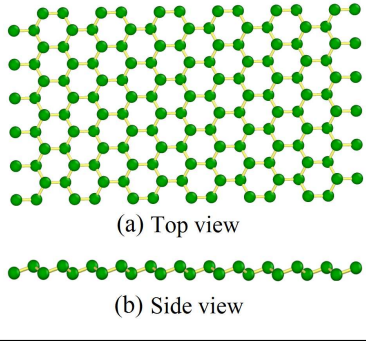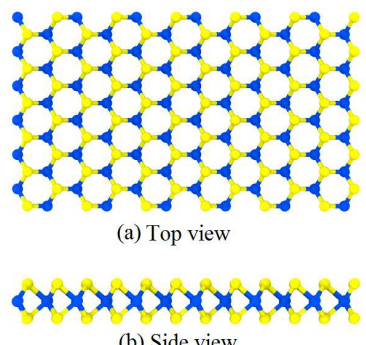


(b)

Figure 1: (a) Three dimensional view of multiplanar hexagonal nano-structures along with side views from two mutually perpendicular directions (b) Top view of multiplanar hexagonal nano-structures

Figure 1 shows a generalized material nano-structure with hexagonal top view, wherein two different atoms are placed in different planes (such as MoS$_2$). There is a different class of materials which has same atoms in the hexagonal nano-structure, but placed in

Table 1: Structural-configuration based classification of hexagonal nano-materials

| Material Type | Structural configuration | Description of nano-materials |
|---|---|---|
| Class A | <br>(a) Top view<br><br>(b) Side view | *Characteristic property from structural point of view*: All the constituent atoms are same and they are in a single plane (e.g. graphene [4, 13]) |
| Class B | <br>(a) Top view<br><br>(b) Side view | *Characteristic property from structural point of view*: The constituent atoms are not same but they are in a single plane (e.g. hBN [15, 17], BCN [18]) |
| Class C | <br>(a) Top view<br><br>(b) Side view | *Characteristic property from structural point of view*: The constituent atoms are same but they are in two different planes (e.g. silicene [19, 20], germanene [21], phosphorene [22], stanene [20, 23], borophene [24]) |
| Class D | <br>(a) Top view<br><br>(b) Side view | *Characteristic property from structural point of view*: The constituent atoms are not same and they are in two different planes (e.g. $MoS_2$ [25], $WS_2$ [26], $MoSe_2$ [27], $WSe_2$ [26], $MoTe_2$ [28]) |

different planes (such as stanene). Other classes of materials have different atoms in the hexagonal nano-structure placed in a single plane (such as hBN) and same atom in the hexagonal nano-structure placed in a single plane (such as graphene). Thus based on nano-structural configurations, the materials with hexagonal nano-structure (top view) can be divided into four classes as presented in Table 1. From structural point of view, the other classes of materials are basically special cases of the materials of Class D. Aim of the present work is to develop generalized closed form analytical formulae for the elastic moduli of such hexagonal multiplanar nano-structures that can be applicable for wide range of materials (Class A to Class D). This paper hereafter is organized as follows: analytical formulae for the elastic moduli of materials with multiplanar hexagonal nano-structures are derived in section 2; results and discussion on the proposed analytical approach is provided in section 3 along with validation of the developed formulae for four different materials belonging to four different classes (graphene, hBN, stanene and $MoS_2$); and finally conclusion and perspective of this work is presented in section 4.

## 2. Elastic properties of hexagonal nano-structures

Generalized closed-form analytical formulae for the elastic moduli of hexagonal multi-planar nano-structures are developed in this section that is applicable to all the materials from Class A to Class D (refer to Table 1). The equivalent elastic properties of atomic bonds are described first, and thereby the closed-form expressions of elastic moduli for generalized multiplaner hexagonal nano-structures are derived. The approach for obtaining the equivalent elastic properties of atomic bonds is well-established in scientific literature [12, 14, 29]. Therefore, the main contributing of this work lies in the later part of this section concerning development of analytical formulae for elastic moduli of multiplanar hexagonal nano-structures. In this context, it can be noted that the mechanics of honeycomb-like structural form is investigated extensively in micro and macro scales based on principles of structural mechanics [30–34].

*2.1. Equivalent elastic properties of atomic bonds*

In nano-scale investigations concerning atomic level behaviour of materials, the total inter-atomic potential energy of a system can be expressed as the sum of different indi-
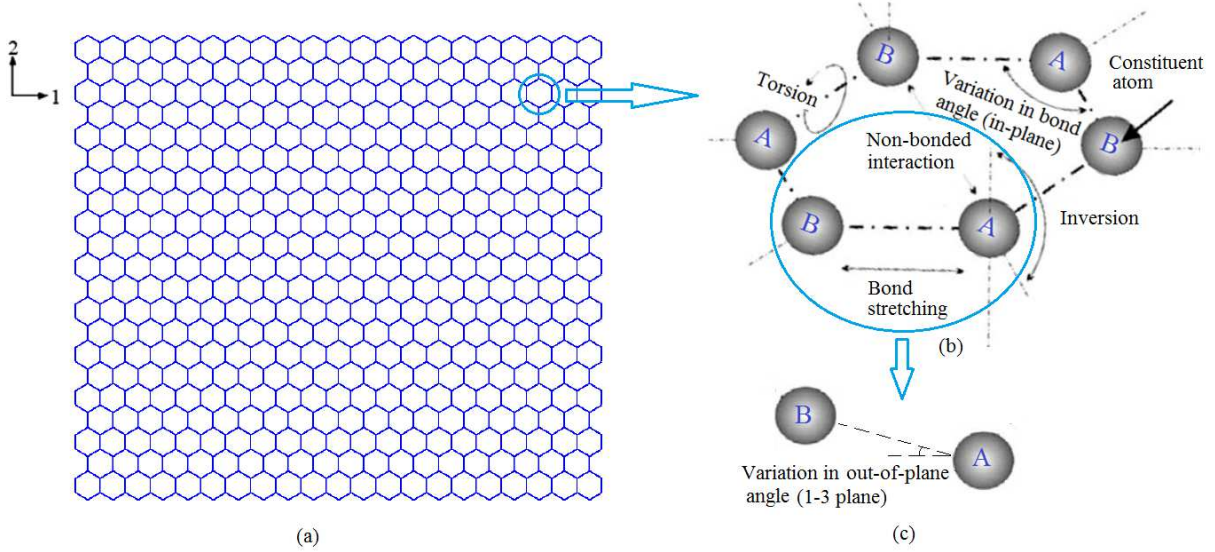
Figure 2: (a) Top view of hexagonal nano-structures (b) Bond structure in hexagonal nano-materials and associated energy components (c) Energy component associated with out-of-plane bending (Direction 1 and 2 are indicated in the figure. Direction 3 is perpendicular to the 1-2 plane.)

vidual energy terms related to bonding and non-bonding interactions [12]. Total strain energy $(E)$ of a nano-structure is the sum of energy contributions from bond stretching $(E_s)$, bending $(E_b)$, torsion $(E_t)$ and energies associated with non-bonded terms $(E_{nb})$ such as the van der Waals attraction, the core repulsions and the coulombic energy (refer to figure 2).

$$E = E_s + E_b + E_t + E_{nb} \qquad (1)$$

Among all the above mentioned energy components, effect of stretching and bending are predominant for small deformation of such nano-structures [14, 29]. However, for the hexagonal nano-structures where the atoms are not in a single plane (materials belonging to Class C and Class D as per Table 1), the strain energy due to bending has two components. Typically the atoms stay in two different planes (/ two symmetric planes with respect to the middle layer) in such material structures and the total bending energy $(E_b)$ consists of in-plane component $(E_{bi})$ and out-of-plane component $(E_{bo})$. Thus the total

6

inter-atomic potential energy $(E)$ can be expressed as

$$E = E_s + E_b$$

$$= E_s + E_{bi} + E_{bo} \tag{2}$$

$$= \frac{1}{2}k_r(\Delta l)^2 + \frac{1}{2}k_\theta(\Delta\theta)^2 + \frac{1}{2}k_\theta(\Delta\alpha)^2$$

where $\Delta l$, $\Delta\theta$ and $\Delta\alpha$ denote the bond elongation, change in in-plane and out-of-plane
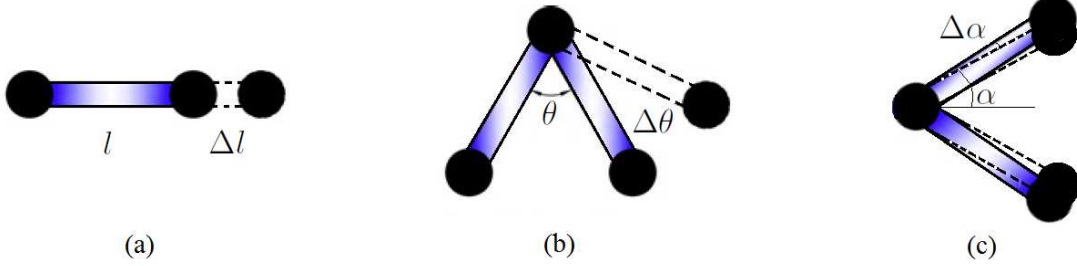


(a)           (b)           (c)

Figure 3: (a) Strain energy due to bond stretching (b) Strain energy due to in-plane angle variation (in 1-2 plane) (c) Strain energy due to out-of-plane angle variation (in 1-3 and 2-3 planes)

angle respectively, as shown in figure 3. $k_r$ and $k_\theta$ are the force constants associated with bond stretching and bending respectively. The first term in the above expression of total inter-atomic potential energy corresponds to strain energy due to stretching $(E_s)$, while the second and third terms represent the strain energies due to in-plane $(E_{bi})$ and out-of-plane $(E_{bo})$ angle variations respectively.

The force constants $(k_r$ and $k_\theta)$ of the bonds between two atoms can be expressed in terms of the member stiffness [35]. According to the standard theory of classical structural mechanics (refer to figure 4), strain energy of a uniform circular beam with cross-sectional area $A$, length $l$, Young's modulus $E$, and second moment of area $I$, under the application of a pure axial force $N$ can be expressed as

$$U_a = \frac{1}{2}\int_0^L \frac{N^2}{EA}\,\mathrm{d}l = \frac{1}{2}\frac{N^2 l}{EA} = \frac{1}{2}\frac{EA}{l}(\Delta l)^2 \tag{3}$$

The strain energies due to pure bending moment $M$ can be written as

$$U_b = \frac{1}{2}\int_0^L \frac{M^2}{EI}\,\mathrm{d}l = \frac{1}{2}\frac{EI}{l}(2\Delta\phi)^2 \tag{4}$$

Comparing Equation 3 with the expression for strain energy due to stretching $(E_s)$ (refer Equation 2), it can be concluded that $K_r = \dfrac{EA}{l}$. For bending, it is reasonable to assume that $2\Delta\phi$ is equivalent to $\Delta\theta$ and $\Delta\alpha$ for in-plane and out-of-plane angle variations re-

7

spectively (refer to figure 4(b)). Thus comparing Equation 4 with the expressions for the strain energies due to in-plane ($E_{bi}$) and out-of-plane ($E_{bo}$) angle variations, the following relation can be obtained: $k_\theta = \dfrac{EI}{l}$. On the basis of the established relationship between molecular mechanics parameters ($k_r$ and $k_\theta$) and structural mechanics parameters ($EA$ and $EI$), the effective elastic moduli of multiplanar hexagonal nano-structures are obtained in the following subsections.
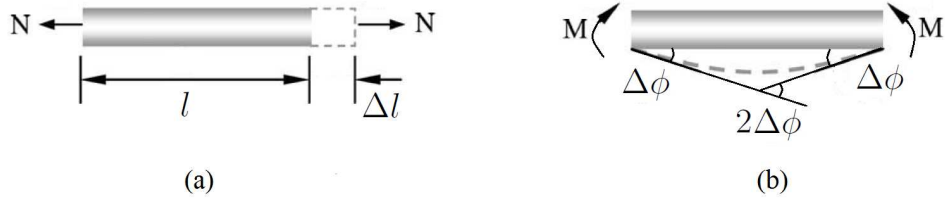


Figure 4: (a) A structural element subjected to pure tension (b) A structural element subjected to pure bending

### 2.2. Young's modulus in direction-1 ($E_1$)

One hexagonal unit cell is considered to derive the expression for Young's moduli of the entire hexagonal periodic nano-structure as shown in figure 5. Because of structural symmetry, horizontal deformation of the unit cell can be obtained by analysing the member AB only. The total horizontal deformation of the member AB (horizontal deflection of one end of the member with respect to the other end) under the application of stress $\sigma_1$ has three components: axial deformation ($\delta_{aH}$), bending deformation due to in-plane loading ($\delta_{bHi}$) and bending deformation due to out-of-plane loading ($\delta_{bHo}$).

$$
\begin{aligned}
\delta_{H11} &= \delta_{aH} + \delta_{bHi} + \delta_{bHo} \\
&= \frac{Hl\cos^2\psi\cos^2\alpha}{AE} + \frac{Hl^3\sin^2\psi}{12EI} + \frac{Hl^3\cos^2\psi\sin^2\alpha}{12EI}
\end{aligned}
\tag{5}
$$

where $A = \dfrac{\pi d^2}{4}$, $I = \dfrac{\pi d^4}{64}$ and $H = \sigma_1 tl(1 + \sin\psi)\cos\alpha$. $l$ and $d$ represent the length and diameter of the member AB respectively. $t$ is the thickness of single layer of such periodic structural form. The three parts of Equation 5 are derived by considering the respective deformation components in direction-1. Figure 5(a) and figure 5(b) show the member AB using top-view and side-view respectively, wherein the horizontal load $H$ acts at the node A in the 1-2 plane. Inclination angle of the member AB in the 1-2 plane and 1-3 plane are

8

$\psi$ and $\alpha$ respectively, as shown in figure 5(e). From figure 5(a) it can be understood that the horizontal force $H$ has two components: $H sin\psi$ (acting in a direction perpendicular to the member AB in the 1-2 plane) and $H cos\psi$ (acting in a direction perpendicular to the force $H sin\psi$ in the 1-2 plane). The $H sin\psi$ component will cause a bending deflection $\Delta_{Hi}$. The component of $\Delta_{Hi}$ in direction-1 is denoted as $\delta_{bHi}$ in Equation 5. Using the standard formula of structural mechanics (bending deflection of one end of a beam with respect to the other end: $\delta = \dfrac{PL^3}{12EI}$, where $L$ is the length of the beam, $P$ is the applied point load across the beam length [36]) the component $\delta_{bHi}$ can be expressed as

$$\delta_{bHi} = \Delta_{Hi} sin\psi = \frac{H sin\psi l^3}{12EI} sin\psi = \frac{H l^3 sin^2\psi}{12EI} \tag{6}$$

The $H cos\psi$ force can be resolved in two different components in the plane perpendicular to the 1-2 plane. The component $H cos\psi cos\alpha$ causes axial deformation of the member AB, while the other component $H cos\psi sin\alpha$ results in the bending deformation $\Delta_{Ho}$ (as indicated in figure 5(b)). The horizontal component of $\Delta_{Ho}$ in the 1-2 plane is denoted as $\delta_{bHo}$ in the Equation 5. Thus we get

$$\delta_{bHo} = \Delta_{Ho} sin\alpha cos\psi = \frac{H cos\psi sin\alpha l^3}{12EI} sin\alpha cos\psi = \frac{H l^3 cos^2\psi sin^2\alpha}{12EI} \tag{7}$$

The horizontal axial deformation component in the 1-2 plane caused by the force $H cos\psi cos\alpha$ is denoted as $\delta_{aH}$ in the Equation 5. Thus we get

$$\delta_{aH} = \frac{H cos\psi cos\alpha l}{AE} cos\psi cos\alpha = \frac{H l cos^2\psi cos^2\alpha}{AE} \tag{8}$$

Using the relationship between molecular mechanics parameters ($k_r$ and $k_\theta$) and structural mechanics parameters ($EA$ and $EI$), form Equation 5, the expression for strain in direction-1 (due to loading in direction-1) can be written as

$$\begin{aligned} \epsilon_{11} &= \frac{\delta_{H11}}{l\cos\psi\cos\alpha} \\ &= \frac{\sigma_1 tl(1 + \sin\psi)}{l\cos\psi} \left( \frac{l^2}{12k_\theta} \left( \sin^2\psi + \cos^2\psi\sin^2\alpha \right) + \frac{\cos^2\psi\cos^2\alpha}{k_r} \right) \end{aligned} \tag{9}$$

On the basis of the basic definition of Young's modulus ($E_1 = \dfrac{\sigma_1}{\epsilon_{11}}$), the closed-form expression for Young's modulus in direction-1 can be obtained as

Figure 5: (a) Free body diagram of member AB for in-plane deformation under the application of horizontal force (b) Free body diagram of member AB for out-of-plane deformation under the application of horizontal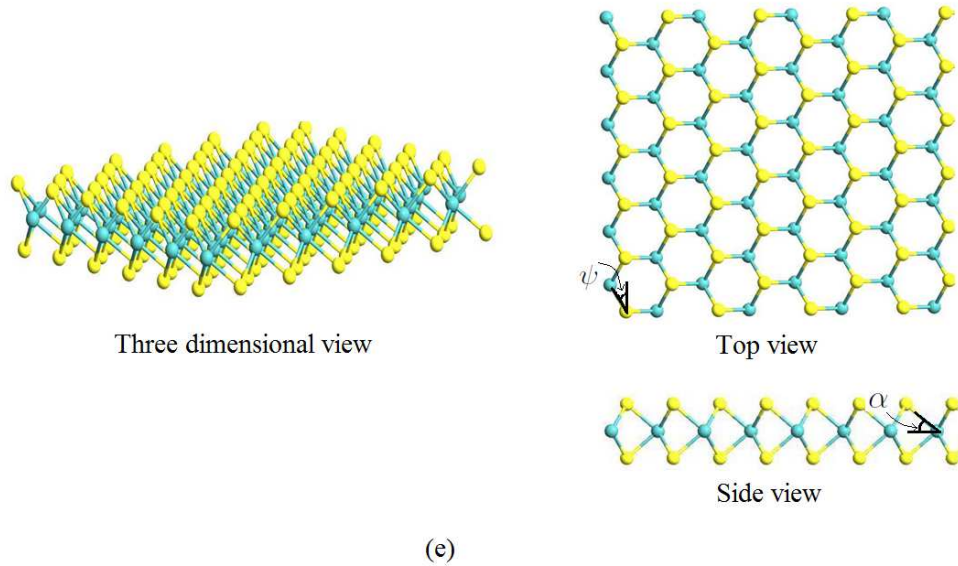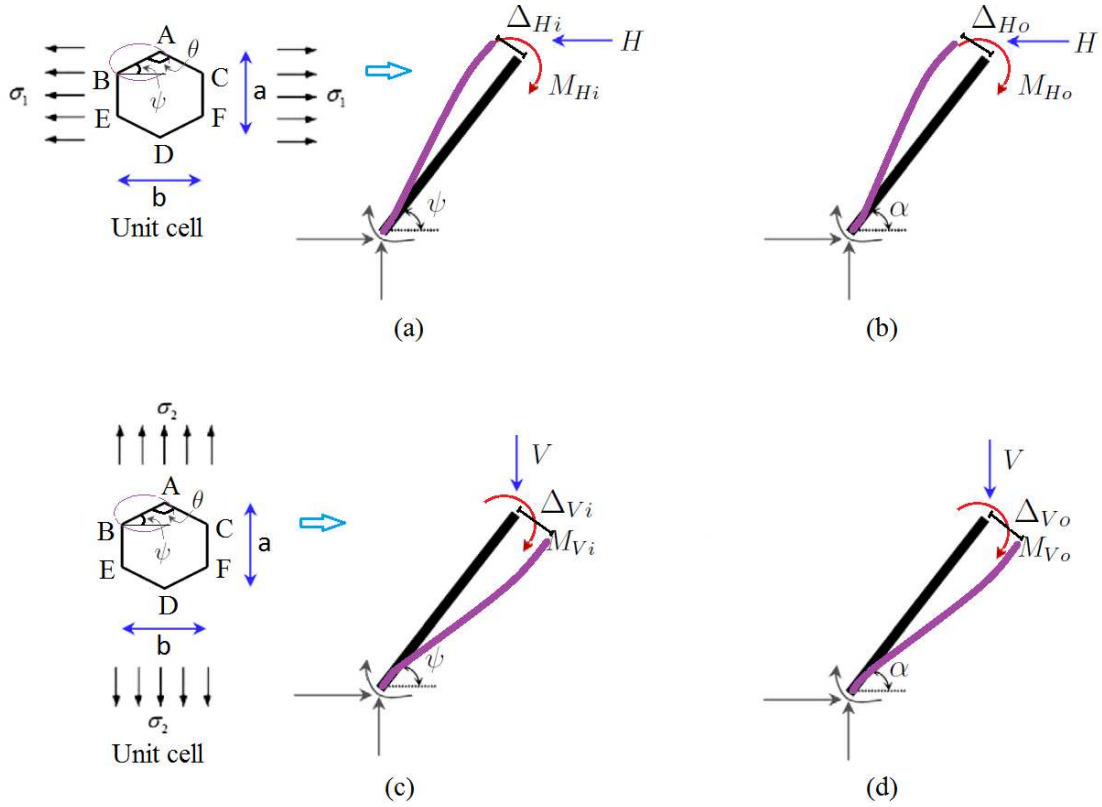 force (c) Free body diagram of member AB for in-plane deformation under the application of vertical force (d) Free body diagram of member AB for out-of-plane deformation under the application of vertical force (e) Three dimensional view of a multiplanar hexagonal nanostructure along with top and side view indicating the in-plane angle ($\psi$) and out-of-plane angle ($\alpha$)

$$E_1 = \frac{\cos\psi}{t(1+\sin\psi)\left(\dfrac{l^2}{12k_\theta}\left(\sin^2\psi + \cos^2\psi\sin^2\alpha\right) + \dfrac{\cos^2\psi\cos^2\alpha}{k_r}\right)} \tag{10}$$

In the above expression $\psi = 90° - \dfrac{\theta}{2}$, where $\theta$ is the bond angle as shown in figure 5.

### 2.3. Young's modulus in direction-2 ($E_2$)

Total vertical deformation of the unit cell under the application of $\sigma_2$ is consisted of the deformation of member AB ($\delta_{V1}$) and member BE ($\delta_{V2}$) in direction-2. Deflection of joint A in direction-2 with respect to joint B has three components: axial deformation ($\delta_{aV1}$), bending deformation due to in-plane loading ($\delta_{bV1i}$) and bending deformation due to out-of-plane loading ($\delta_{bV1o}$).

$$\begin{aligned}
\delta_{V1} &= \delta_{aV1} + \delta_{bV1i} + \delta_{bV1o} \\
&= \frac{Vl\sin^2\psi\cos^2\alpha}{AE} + \frac{Vl^3\cos^2\psi}{12EI} + \frac{Vl^3\sin^2\psi\sin^2\alpha}{12EI}
\end{aligned} \tag{11}$$

where $V = \sigma_2 t l \cos\psi\cos\alpha$. As the member BE is parallel to the 2-3 plane, deflection of joint B with respect to the joint E has two components: axial deformation ($\delta_{aV2}$) and bending deformation due to out-of-plane loading ($\delta_{bV2o}$). It can be noted that the force acting on the member BE is $2V$ as there are similar unit cells adjacent to the one being analysed.

$$\begin{aligned}
\delta_{V2} &= \delta_{aV2} + \delta_{bV2o} \\
&= \frac{2Vl\cos^2\alpha}{AE} + \frac{2Vl^3\sin^2\alpha}{12EI}
\end{aligned} \tag{12}$$

Replacing the expressions of $V$, $A$, $I$, $AE$ and $EI$, the total deformation in direction-2 can be obtained from Equation 11 and 12 as

$$\begin{aligned}
\delta_{V22} &= \delta_{V1} + \delta_{V2} \\
&= \sigma_2 t l \cos\psi\cos\alpha \left(\frac{l^2}{12k_\theta}\left(\cos^2\psi + \sin^2\psi\sin^2\alpha + 2\sin^2\alpha\right) + \frac{\cos^2\alpha}{k_r}\left(\sin^2\psi + 2\right)\right)
\end{aligned} \tag{13}$$

From Equation 13, the strain in direction-2 (due to loading in direction-2) can be expresses as

$$
\begin{aligned}
\epsilon_{22} &= \frac{\delta_{V22}}{(l + l \sin \psi) \cos \alpha} \\
&= \frac{\sigma_2 t \cos \psi}{1 + \sin \psi} \left( \frac{l^2}{12 k_\theta} \left( \cos^2 \psi + \sin^2 \psi \sin^2 \alpha + 2 \sin^2 \alpha \right) + \frac{\cos^2 \alpha}{k_r} \left( \sin^2 \psi + 2 \right) \right)
\end{aligned}
\tag{14}
$$

On the basis of the basic definition of Young's modulus ($E_2 = \dfrac{\sigma_2}{\epsilon_{22}}$), the closed-form expression for Young's modulus in direction-2 can be obtained as

$$
E_2 = \frac{1 + \sin \psi}{t \cos \psi \left( \dfrac{l^2}{12 k_\theta} \left( \cos^2 \psi + \sin^2 \psi \sin^2 \alpha + 2 \sin^2 \alpha \right) + \dfrac{\cos^2 \alpha}{k_r} \left( \sin^2 \psi + 2 \right) \right)}
\tag{15}
$$

In the above expression $\psi = 90° - \dfrac{\theta}{2}$, where $\theta$ is the bond angle as shown in figure 5. Thus the Young's moduli of a material with hexagonal nano-structure can be predicted using the closed-form formulae (Equation 10 and 15) from molecular mechanics parameters ($k_r$ and $k_\theta$), bond length ($l$), bond angle ($\theta$) and out-of-plane angle ($\alpha$), which are available in the molecular mechanics literature.

*2.4. Poisson's ratio $\nu_{12}$*

Poisson's ratio for the loading direction-1 ($\nu_{12}$) can be obtained as

$$
\nu_{12} = -\frac{\epsilon_{12}}{\epsilon_{11}}
\tag{16}
$$

where $\epsilon_{12}$ and $\epsilon_{11}$ are the strains in direction-2 and direction-1 respectively due to loading in direction-1. The expression for $\epsilon_{11}$ is given in Equation 9. Derivation for the expression of $\epsilon_{12}$ is provided next. The deformation in direction-2 due to loading in direction-1 can be obtained by considering one hexagonal unit cell as shown in figure 5. Because of structural symmetry, deformation in direction-2 of the unit cell due to loading in direction-1 can be obtained by analysing the member AB only. The total deformation in direction-2 of the member AB (deflection in direction-2 of one end of the member with respect to the other end) under the application of stress $\sigma_1$ has two components: bending deformation due to

in-plane loading ($\delta_{bVi1}$) and bending deformation due to out-of-plane loading ($\delta_{bVo1}$).

$$
\begin{aligned}
\delta_{H12} &= \delta_{bVi1} + \delta_{bVo1} \\
&= -\frac{Hl^3 \sin\psi \cos\psi}{12EI} + \frac{Hl^3 \sin\psi \cos\psi \sin^2\alpha}{12EI} \\
&= -\frac{Hl^3 \sin\psi \cos\psi \cos^2\alpha}{12EI}
\end{aligned}
\tag{17}
$$

Using the relationship between molecular mechanics parameter $k_\theta$ and structural mechanics parameter $EI$, form Equation 17, the expression for strain in direction-2 (due to loading in direction-1) can be written as

$$
\begin{aligned}
\epsilon_{12} &= \frac{\delta_{H12}}{(l + l\sin\psi)\cos\alpha} \\
&= -\frac{Hl\sin\psi \cos\psi \cos\alpha}{12k_\theta (1 + \sin\psi)}
\end{aligned}
\tag{18}
$$

On the basis of the basic definition of $\nu_{12}$ as shown in Equation 16, the closed-form expression of Poisson's ratio for the loading direction-1 can be obtained as

$$
\nu_{12} = \frac{\sin\psi \cos^2\psi \cos^2\alpha\, l^2}{12k_\theta (1 + \sin\psi)\left(\dfrac{l^2}{12k_\theta}\left(\sin^2\psi + \cos^2\psi \sin^2\alpha\right) + \dfrac{\cos^2\psi \cos^2\alpha}{k_r}\right)}
\tag{19}
$$

In the above expression $\psi = 90° - \dfrac{\theta}{2}$, where $\theta$ is the bond angle as shown in figure 5.

### 2.5. Poisson's ratio $\nu_{21}$

Poisson's ratio for the loading direction-2 ($\nu_{21}$) can be obtained as

$$
\nu_{21} = -\frac{\epsilon_{21}}{\epsilon_{22}}
\tag{20}
$$

where $\epsilon_{21}$ and $\epsilon_{22}$ are the strains in direction-1 and direction-2 respectively due to loading in direction-2. The expression for $\epsilon_{22}$ is given in Equation 14. Derivation for the expression of $\epsilon_{21}$ is provided next. The deformation in direction-1 due to loading in direction-2 can be obtained by considering one hexagonal unit cell as shown in figure 5. Because of structural symmetry, deformation in direction-1 of the unit cell due to loading in direction-2 can be obtained by analysing the member AB only. The total deformation in direction-1 of the member AB (deflection in direction-1 of one end of the member with respect to the other end) under the application of stress $\sigma_2$ has two components: bending deformation due to

in-plane loading ($\delta_{bHi2}$) and bending deformation due to out-of-plane loading ($\delta_{bHo2}$).

$$
\begin{aligned}
\delta_{H21} &= \delta_{bHi2} + \delta_{bHo2} \\
&= -\frac{Vl^3 \sin\psi\cos\psi}{12EI} + \frac{Vl^3 \sin\psi\cos\psi \sin^2\alpha}{12EI} \\
&= -\frac{Vl^3 \sin\psi\cos\psi\cos^2\alpha}{12EI}
\end{aligned}
\tag{21}
$$

Using the relationship between molecular mechanics parameter $k_\theta$ and structural mechanics parameter $EI$, form Equation 21, the expression for strain in direction-1 (due to loading in direction-2) can be written as

$$
\begin{aligned}
\epsilon_{21} &= \frac{\delta_{H21}}{l\cos\psi\cos\alpha} \\
&= -\frac{Vl\sin\psi\cos\alpha}{12k_\theta}
\end{aligned}
\tag{22}
$$

On the basis of the basic definition of $\nu_{21}$ as shown in Equation 20, the closed-form expression of Poisson's ratio for the loading direction-2 can be obtained as

$$
\nu_{21} = \frac{\sin\psi\,(1+\sin\psi)\cos^2\alpha\, l^2}{12k_\theta\left(\dfrac{l^2}{12k_\theta}\left(\cos^2\psi+\sin^2\psi\sin^2\alpha+2\sin^2\alpha\right)+\dfrac{\cos^2\alpha}{k_r}\left(\sin^2\psi+2\right)\right)}
\tag{23}
$$

In the above expression $\psi = 90° - \dfrac{\theta}{2}$, where $\theta$ is the bond angle as shown in figure 5.

### 2.6. Remark 1: Reciprocal theorem

From the Equation 10, Equation 15, Equation 19 and Equation 23, it can be noticed that the reciprocal theorem is obeyed for multiplanar hexagonal nanostructures

$$
E_1\nu_{21} = E_2\nu_{12} = \frac{\sin\psi\cos\psi\cos^2\alpha\, l^2\left(\dfrac{l^2}{12k_\theta}\left(\sin^2\psi+\cos^2\psi\sin^2\alpha\right)+\dfrac{\cos^2\psi\cos^2\alpha}{k_r}\right)^{-1}}{12k_\theta t\left(\dfrac{l^2}{12k_\theta}\left(\cos^2\psi+\sin^2\psi\sin^2\alpha+2\sin^2\alpha\right)+\dfrac{\cos^2\alpha}{k_r}\left(\sin^2\psi+2\right)\right)}
\tag{24}
$$

The above equation implies that only (any) three of the four elastic moduli $E_1$, $E_2$, $\nu_{12}$ and $\nu_{21}$ are independent.

### 2.7. Remark 2: Non-dimensionalization

The physics based analytical formulae developed in this article are capable of providing an in-depth understanding of the behaviour of multiplanar hexagonal nano-structures.

Non-dimesional quantities in physical systems can cater to an insight for wide range of nano-scale materials. The expressions for the two Young's moduli (as presented in Equation 10 and 15) and the two Poisson's ratios (as presented in Equation 19 and 23) can be rewritten in terms of non-dimensional parameters as

$$\tilde{E}_1 = \frac{\cos\psi}{(1+\sin\psi)\left(\lambda\left(\sin^2\psi + \cos^2\psi\sin^2\alpha\right) + \cos^2\psi\cos^2\alpha\right)} \tag{25}$$

$$\tilde{E}_2 = \frac{1+\sin\psi}{\cos\psi\left(\lambda\left(\cos^2\psi + \sin^2\psi\sin^2\alpha + 2\sin^2\alpha\right) + \cos^2\alpha\left(\sin^2\psi + 2\right)\right)} \tag{26}$$

$$\tilde{\nu}_{12} = \frac{\sin\psi\cos^2\psi\cos^2\alpha\lambda}{(1+\sin\psi)\left(\lambda\left(\sin^2\psi + \cos^2\psi\sin^2\alpha\right) + \cos^2\psi\cos^2\alpha\right)} \tag{27}$$

$$\tilde{\nu}_{21} = \frac{\sin\psi\left(1+\sin\psi\right)\cos^2\alpha\lambda}{\left(\lambda\left(\cos^2\psi + \sin^2\psi\sin^2\alpha + 2\sin^2\alpha\right) + \cos^2\alpha\left(\sin^2\psi + 2\right)\right)} \tag{28}$$

where $\lambda$ $\left(= \dfrac{l^2}{12}\dfrac{k_r}{k_\theta}\right)$ is a non-dimensional aspect ratio measure of the bonds that is found to vary in the range of 0.4 to 2.8 for common materials with hexagonal nano-structures. It is interesting to notice that $\lambda$ reduces to $\dfrac{4}{3}\left(\dfrac{l}{d}\right)^2$ using the definition of $k_r$ and $k_\theta$, where $l$ and $d$ are the bond length and bond diameter respectively. Thus the parameter $\lambda$ is a measure of the aspect ratio of the bonds in hexagonal nano-structure. $\tilde{E}_1 = \dfrac{E_1 t}{k_r}$ and $\tilde{E}_2 = \dfrac{E_2 t}{k_r}$ are non-dimensional representation of the Young's moduli. $\tilde{\nu}_{12}$ $(= \nu_{12})$ and $\tilde{\nu}_{21}$ $(= \nu_{21})$ are the non-dimensional Poisson's ratios. Thus it is interesting to notice that the non-dimensional elastic moduli depend on the aspect ratio of the bond, in-plane angle and out-of-plane angles only. Results are presented in section 3 considering the non-dimensional quantities for in-depth mechanical characterization of hexagonal nano-structures.

2.8. Remark 3: Special cases

For the hexagonal nano-structures belonging to Class A and Class B, $\alpha = 0$. Thus Equation 10 and 15 for the materials of Class A and Class B reduce to

$$E_1 = \frac{\cos\psi}{t(1+\sin\psi)\left(\dfrac{l^2}{12k_\theta}\sin^2\psi + \dfrac{\cos^2\psi}{k_r}\right)} \tag{29}$$

$$E_2 = \frac{1 + \sin \psi}{t \cos \psi \left( \dfrac{l^2}{12k_\theta} \cos^2 \psi + \dfrac{\left( \sin^2 \psi + 2 \right)}{k_r} \right)} \tag{30}$$

However, for regular hexagonal nano-structures (such as graphene), the bond angle ($\theta$) is 120°. Thus replacing $\psi = 30°$, the Equation 29 and 30 yield to

$$E_1 = E_2 = \frac{4\sqrt{3}k_r k_\theta}{t \left( \dfrac{k_r l^2}{4} + 9k_\theta \right)} \tag{31}$$

The above expression matches with the formula provided by Shokrieh and Rafiee [14] for graphene.

Similarly, for the hexagonal nano-structures belonging to Class A and Class B, the Poisson's ratios can be expressed as (substituting $\alpha = 0$ in Equation 19 and 23)

$$\nu_{12} = \frac{\sin \psi \cos^2 \psi l^2}{12k_\theta \left( 1 + \sin \psi \right) \left( \dfrac{l^2}{12k_\theta} \sin^2 \psi + \dfrac{\cos^2 \psi}{k_r} \right)} \tag{32}$$

$$\nu_{21} = \frac{\sin \psi \left( 1 + \sin \psi \right) l^2}{12k_\theta \left( \dfrac{l^2}{12k_\theta} \cos^2 \psi + \dfrac{\left( \sin^2 \psi + 2 \right)}{k_r} \right)} \tag{33}$$

However, for regular hexagonal nano-structures (such as graphene), the bond angle ($\theta$) is 120°. Thus replacing $\psi = 30°$, the Equation 32 and 33 yield to

$$\nu_{12} = \nu_{21} = \frac{1}{1 + \dfrac{36k_\theta}{k_r l^2}} \tag{34}$$

It can be noted that the analytical expressions of Poisson's ratios, even for graphene-like hexagonal structures, are first provided in Equation 34 that can be applicable to the materials of Class A and Class B.

## 3. Results and discussion

Four different materials with hexagonal nano-structures are considered (graphene, hBN, stanene and $MoS_2$) that belong to four different classes as categorized in Table 1. To validate the analytical formulae of elastic moduli derived in the preceding section, the results are compared with previous studies reported in scientific literature (experimental,

ab-initio, molecular dynamics and molecular mechanics, as available). The proposed expressions for elastic moduli are generalized in nature and they can be applicable for wide range of materials with hexagonal nano-structural forms by providing respective structural parameters as input. Comparative results for the two Young's moduli are presented in Table 2 as $\bar{E}_1 = E_1 \times t$ and $\bar{E}_2 = E_2 \times t$ (tensile rigidity), where $t$ is the single layer thickness [12, 15]. Thus the values of Young's moduli ($E_1$ and $E_2$ in TPa) can be obtained by dividing the presented values ($\bar{E}_1$ and $\bar{E}_2$ with unit TPa-nm) by the respective single layer thickness ($t$ in nm). Single layer thickness of the four considered materials are indicated in the following paragraphs. Comparative results for the two Poisson's ratio are presented in Table 3. Good agreement between the results obtained using the derived closed-form formulae and the results from scientific literature for all the four classes of material corroborates the validity of the proposed analytical approach.

Graphene belongs to the Class A according to structural configuration, wherein all the atoms are carbon and they are in a single plane. The molecular mechanics parameters $k_r$ and $k_\theta$ can be obtained from literature using AMBER force filed [37] as $k_r = 938$ kcal mol$^{-1}$nm$^{-2}$ = $6.52 \times 10^{-7}$ Nnm$^{-1}$ and $k_\theta = 126$ kcal mol$^{-1}$rad$^{-2}$ = $8.76 \times 10^{-10}$ Nnm rad$^{-2}$. The out-of-plane angle for graphene is $\alpha = 0$ and the bond angle is $\theta = 120°$ (i.e. $\psi = 30°$), while bond length and thickness of single layer graphene can be obtained from literature as 0.142 nm and 0.34 nm respectively [13]. The value of Young's moduli obtained using the proposed expressions are: $E_1 = E_2 = 1.0419$ TPa, which is quite in good agreement with available literature [10, 12–14, 38–44] (refer to Table 2).

Hexagonal boron nitride (hBN) belongs to the Class B according to structural configuration, wherein two different atoms B and N form the material structure but they are in a single plane. The molecular mechanics parameters $k_r$ and $k_\theta$ can be obtained from literature using DREIDING force model [73] as $k_r = 4.865 \times 10^{-7}$ Nnm$^{-1}$ and $k_\theta = 6.952 \times 10^{-10}$ Nnm rad$^{-2}$ [17]. The out-of-plane angle for hBN is $\alpha = 0$ and the bond angle is $\theta = 120°$ (i.e. $\psi = 30°$), while bond length and thickness of single layer hBN can be obtained from literature as 0.145 nm and 0.098 nm respectively [15]. The value of tensile rigidity (Young's modulus multiplied by thickness) obtained using the proposed expressions are: $\bar{E}_1 = \bar{E}_2 = 0.2659$ TPa-nm, which are quite in good agreement with available literature

17

Table 2: Results for Young's moduli of single layer materials with four different classes of nano-structure as described in Table 1 (results are presented as $\bar{E}_1 = E_1 \times t$ and $\bar{E}_2 = E_2 \times t$, where $t$ is the single layer thickness of a particular nano-material)

| Material | Present Results (TPa-nm) | Reference results from literature ($\bar{E}_1 = \bar{E}_2$) (TPa-nm) |
|---|---|---|
| Graphene (Class A) | $\bar{E}_1 = 0.3542$ $\bar{E}_2 = 0.3542$ | Experimental: $0.34 \pm 0.034$ [38], 0.272–0.306 [39] <br> Ab initio: 0.350 [40], 0.357 [10], 0.377 [41], 0.364 [42] <br> Molecular Dynamics: 0.357 [43], $0.343 \pm 0.01$ [44] <br> Molecular Mechanics: 0.354 [14], 0.3604 [12] |
| hBN (Class B) | $\bar{E}_1 = 0.2659$ $\bar{E}_2 = 0.2659$ | Experimental: $0.251 \pm 0.015$ [45] <br> Ab initio: 0.271 [40], 0.272 [46] <br> Molecular Dynamics: 0.236 [47], 0.278 [48] <br> Molecular Mechanics: 0.269 [49], 0.322 [50] |
| Stanene (Class C) | $\bar{E}_1 = 0.0545$ $\bar{E}_2 = 0.0643$ | Experimental: – <br> Ab initio: 0.0528 [51] <br> Molecular Dynamics: – <br> Molecular Mechanics: – |
| $MoS_2$ (Class D) | $\bar{E}_1 = 0.1073$ $\bar{E}_2 = 0.2141$ | Experimental: $0.211 \pm 0.012$ [52], $0.1629 \pm 0.0603$ [53] <br> Ab initio: 0.141 [54], 0.262 [55] <br> Molecular Dynamics: 0.150 [56] <br> Molecular Mechanics: – |

Table 3: Results for Poisson's ratios of single layer materials with four different classes of nano-structure as described in Table 1

| Material | Present Results | Reference results from literature |
|---|---|---|
| Graphene (Class A) | $\nu_{12} = 0.2942$ <br><br> $\nu_{21} = 0.2942$ | Experimental: 0.165 [57] <br><br> Ab initio: 0.12–0.16 [58], 0.186 [59], 0.34 [60] <br><br> Molecular Dynamics: 0.17 [61], 0.41 [62] <br><br> Molecular Mechanics: 0.11–0.12 [63], 0.195 [64], 0.653–0.848 [13], 1.129–1.1441 [65] |
| hBN (Class B) | $\nu_{12} = 0.2901$ <br><br> $\nu_{21} = 0.2901$ | Experimental: – <br><br> Ab initio: 0.2–0.3 [66], 0.211 [67], 0.2–0.24 [66], 0.13–0.16 [68] <br> Molecular Dynamics: – <br><br> Molecular Mechanics: 0.384–0.389 [69], 0.400–0.405 [69], 0.384–0.389 [69], 0.211 [69], 0.053 [69], 0.2–0.4 [70] |
| Stanene (Class C) | $\nu_{12} = 0.1394$ <br><br> $\nu_{21} = 0.1645$ | Experimental: – <br><br> Ab initio: – <br><br> Molecular Dynamics: – <br><br> Molecular Mechanics: – |
| $MoS_2$ (Class D) | $\nu_{12} = 0.0690$ <br><br> $\nu_{21} = 0.1376$ | Experimental: – <br><br> Ab initio: 0.21 [71] <br><br> Molecular Dynamics: 0.29 [72] <br><br> Molecular Mechanics: – |

[15, 40, 45–47, 49, 50, 74–77] (refer to Table 2).

Stanene belongs to the Class C according to structural configuration, wherein all the atoms are Sn but they are in two different planes. The molecular mechanics parameters $k_r$ and $k_\theta$ can be obtained from literature as $k_r = 0.85 \times 10^{-7}$ Nnm$^{-1}$ and $k_\theta = 1.121 \times 10^{-9}$ Nnm rad$^{-2}$ [51, 78]. The out-of-plane angle for stanene is $\alpha = 17.5°$ and the bond angle is $\theta = 109°$ (i.e. $\psi = 35.5°$), while bond length and thickness of single layer stanene can be obtained from literature as 0.283 nm and 0.086 nm respectively [51, 78–80]. Published studies concerning the Young's moduli of stanene is very scarce in scientific literature. Thus the presented values of Young's moduli in this paper can serve as future references. The in-plane stiffness of stanene reported by Modarresi *et al.* [51] is 0.04 TPa-nm irrespective of any direction. However, it should be noted that the in-plane stiffness of a material having hexagonal nano-structure depends on the direction of applied stress according to its definition. In-plane stiffness of a material can be defined as follows: $F = \dfrac{EA}{L}\Delta L = k\Delta L$, where $k$ $(= \dfrac{EA}{L})$ is the in-plane stiffness. Here $L$ and $\Delta L$ represent the length of the material along the direction of applied stress and elongation in that direction respectively. $E$ denotes the Young's modulus along the direction of applied stress. $A$ is the cross-sectional area for applied stress. Thus, considering the unit cell shown in figure 5, the in-plane stiffness in direction-1 and direction-2 (refer to figure 2 for directions) can be expressed as: $k_1 = E_1 t \left(\dfrac{a}{b}\right) = \bar{E}_1 \left(\dfrac{a}{b}\right)$ and $k_2 = E_2 t \left(\dfrac{b}{a}\right) = \bar{E}_2 \left(\dfrac{b}{a}\right)$ respectively. For stanene the parameters $a$ and $b$ can be calculated from the bond length and in-plane angle as: $a = 0.61$ nm and $b = 0.46$ nm. The value of Young's moduli from the proposed expressions are: $E_1 = 0.3166$ TPa and $E_2 = 0.3736$ TPa, thereby the tensile rigidity (Young's modulus multiplied by thickness) in the two directions can be obtained as: $\bar{E}_1 = 0.0545$ TPa-nm and $\bar{E}_2 = 0.0643$ TPa-nm. As per the above discussion, the in-plane stiffness can be obtained from the proposed expressions as: $k_1 = 0.0723$ TPa-nm and $k_2 = 0.0484$ TPa-nm. Thus the in-plane stiffness in direction-2 calculated using the present formulae is quite close to the values provided by Modarresi *et al.* [51], wherein the results are reported presumably considering the direction-2 (refer to Table 2).

Molybdenum disulfide (MoS$_2$) belongs to the Class D according to structural configuration, wherein two different atoms Mo and S form the material structure and they are

in two different planes. The molecular mechanics parameters $k_r$ and $k_\theta$ can be obtained from literature as $k_r = 1.646 \times 10^{-7}$ Nnm$^{-1}$ and $k_\theta = 1.677 \times 10^{-9}$ Nnm rad$^{-2}$, while the out-of-plane angle, bond angle, bond length and thickness of single layer MoS$_2$ are $\alpha = 48.15°$, $\theta = 82.92°$ (i.e. $\psi = 48.54°$), 0.242 nm and 0.6033 nm respectively [25, 81–85]. The value of tensile rigidity (Young's modulus multiplied by thickness) obtained using the proposed expressions are: $\bar{E}_1 = 0.1073$ and $\bar{E}_2 = 0.2141$ TPa-nm, which are quite in good agreement with available literature [52–56, 86] (refer to Table 2).

The results for Poisson's ratios obtained from the proposed analytical formulae are provided in Table 3 along with reference values from literature. The reported values in literature for graphene and hBN show wide range of variability, while the reference values of Poisson's ratios for stanene and MoS$_2$ are very scarce in the scientific literature. The results obtained using the proposed formulae agree well with majority of the reported values for Poisson's ratios. However, it is noteworthy that for graphene and hBN $\nu_{12} = \nu_{21}$, while for stanene and MoS$_2$ $\nu_{12} < \nu_{21}$. The reciprocal theorem is satisfied perfectly for all the four classes of materials.

The physics based analytical formulae presented in this article are capable of providing a thorough insight regarding the behaviour of multiplanar hexagonal nano-structures representing wide range of materials. Variations of the two non-dimensional Young's moduli ($\tilde{E}_1$ and $\tilde{E}_2$) and the two Poisson's ratios with in-plane and out-of-plane angles ($\theta$ and $\alpha$) for different values of the aspect ratio measure ($\lambda$) are presented in figure 6 and 7 using the non-dimensional parameters as described in subsection 2.7. The aspect ratio measure of the bonds ($\lambda$) varies in the range of 0.4 to 2.8 for common materials with hexagonal nano-structures (specifically in case of the four considered materials: $\lambda = 1.2507, 2.495, 0.5061, 0.479$ for graphene, hBN, stanene and MoS$_2$ respectively). It is observed that the sensitivity of the out-of-plane angle is lesser compared to in-plane angle for both the non-dimensional Young's moduli on the basis of the slopes in two perpendicular directions of the surface plots. Such plots can readily provide the idea about the elastic moduli of any material with hexagonal nano-structure in a comprehensive manner; exact values of the elastic moduli can be easily obtained using the proposed computationally efficient closed-form formulae.
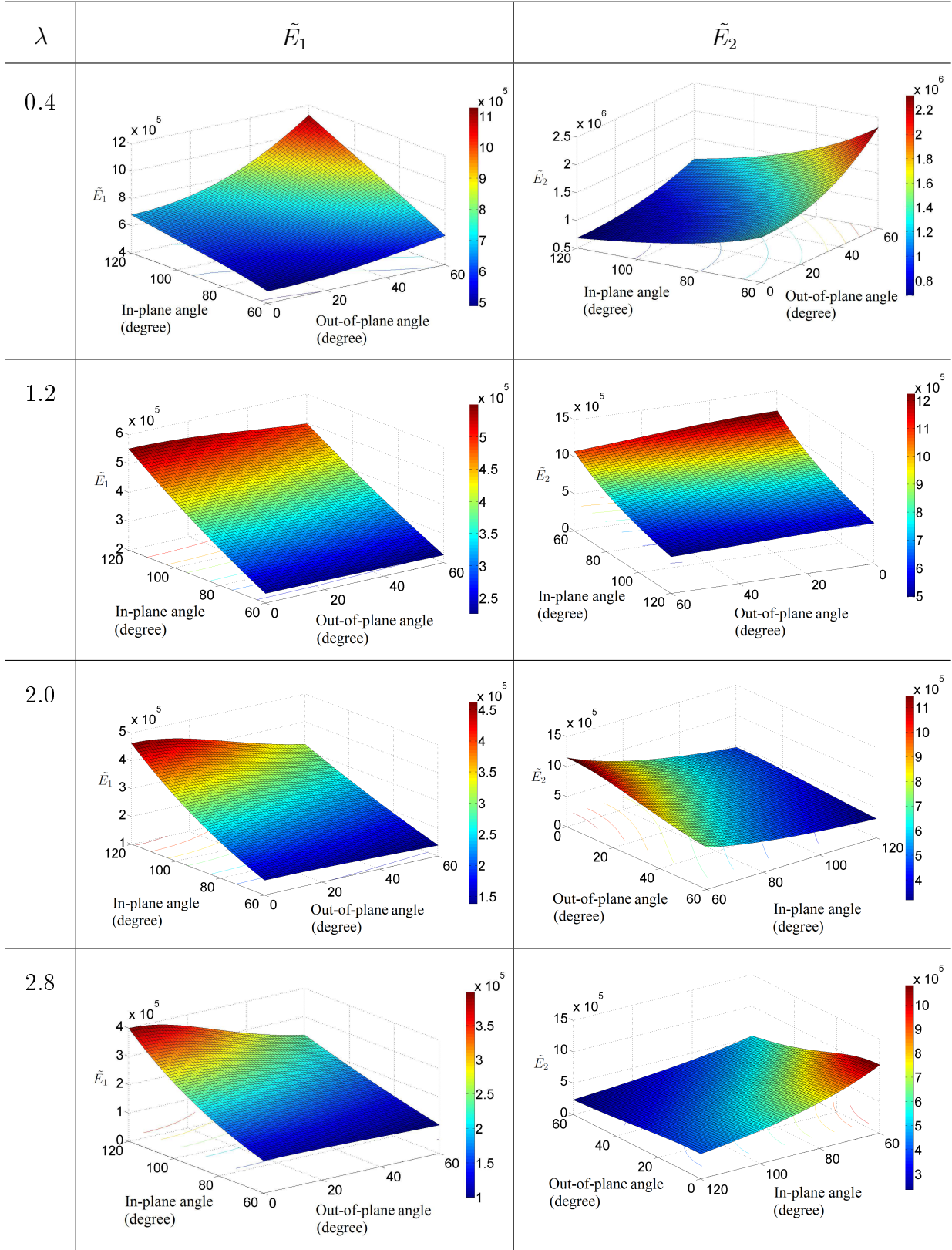
Figure 6: Variation of Young's moduli with in-plane bond angle ($\theta$) and out-of-plane angle ($\alpha$). Here $\lambda = \dfrac{l^2 k_r}{12 k_\theta}$, $\tilde{E}_1 = \dfrac{E_1 t}{k_r}$, $\tilde{E}_2 = \dfrac{E_2 t}{k_r}$, where $l$ and $t$ are the bond length and single layer thickness.
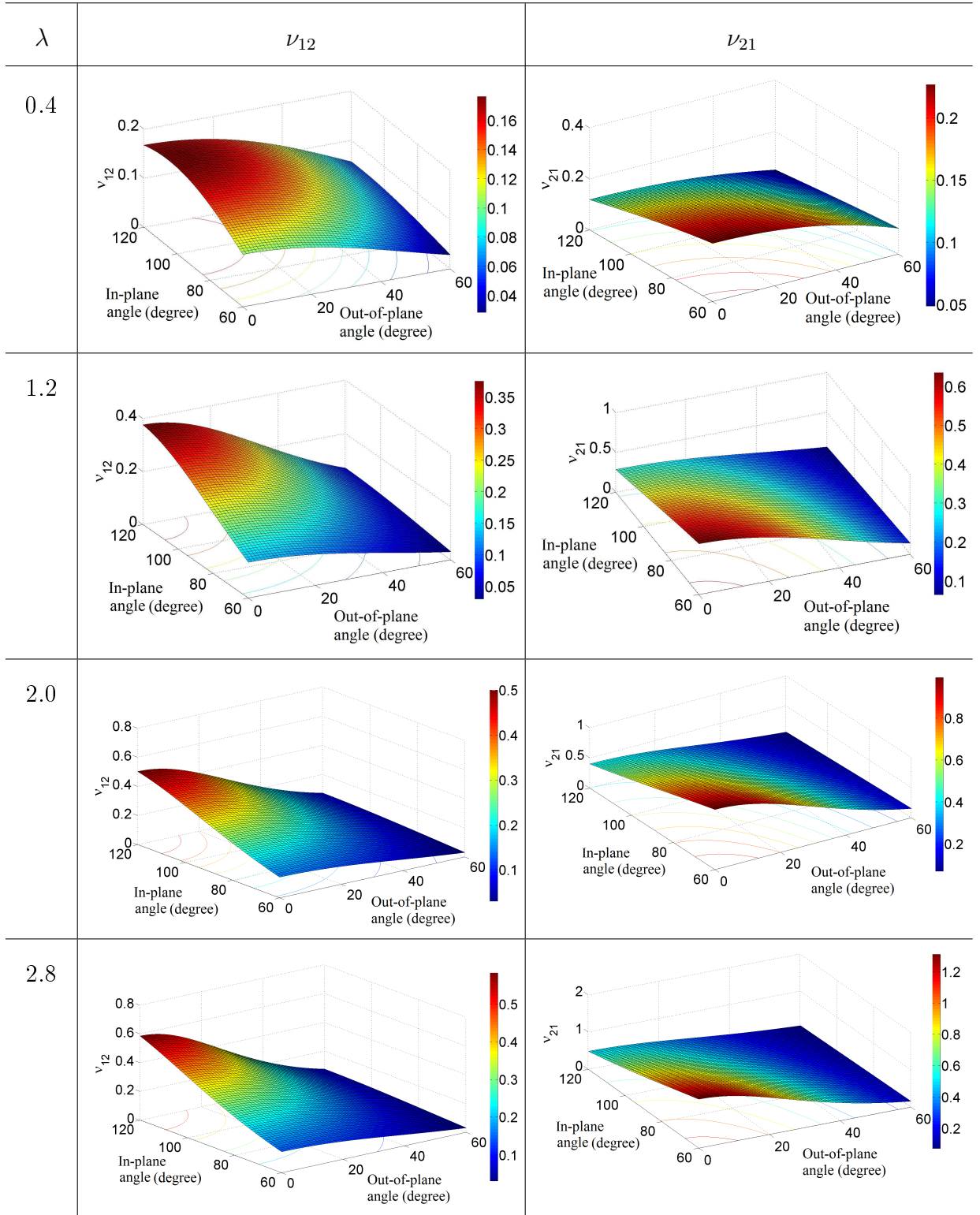
Figure 7: Variation of Poisson's ratios ($\tilde{\nu}_{12} = \nu_{12}$ and $\tilde{\nu}_{21} = \nu_{21}$) with in-plane bond angle ($\theta$), out-of-plane angle ($\alpha$) and $\lambda$ ($= \dfrac{l^2 k_r}{12 k_\theta}$)

It is interesting to notice from the presented results that for graphene and hBN, $E_1 = E_2$ and $\nu_{12} = \nu_{21}$, while for stanene and $MoS_2$, $E_1 < E_2$ and $\nu_{12} < \nu_{21}$. In a broader sense, materials having regular hexagonal nano-structures with $\theta = 120°$ and $\alpha = 0°$ ( Class A and Class B) have equal value of elastic modulus in two perpendicular directions. However, for materials belonging to Class C and Class D, the elastic modulus for direction-2 is more than that of direction-1, even though the difference is not significant. Similar trend is found to be reported for $MoS_2$ by Li [87]. A major contribution of this article is development of the generalized closed-form formulae for hexagonal nano-structures having the atoms in multiple planes. Mechanical properties such as Young's moduli and Poisson's ratios are of utmost importance for accessing the viability of their use in various applications of nanoelectromechanical systems. The formulae for elastic moduli presented in this article can serve as an efficient reference for any nano-scale material having hexagonal structural form.

## 4. Conclusion

Generalized closed-form analytical formulae for the elastic moduli of hexagonal multiplanar nano-structures are developed in this article. From the nano-structural point of view, the materails having hexagonal structural forms are categorized in four different classes. The proposed analytical formulae are applicable to all the classes of material. Four different materials belonging to the four different classes (graphene, hBN, stanene and $MoS_2$) are considered to present results based on the analytical approach. Good agreement in the results obtained from the derived analytical expressions and scientific literature corroborates the validity of the proposed formulae. The physics based analytical formulae developed in this article are capable of providing a comprehensive in-depth insight regarding the behaviour of such multiplanar hexagonal nano-structures. The effect of variation in in-plane and out-of-plane angles to the elastic moduli of materials are investigated using the closed-form formulae based on non-dimensional parameters. An attractive feature of the analytical approach is that it is computationally efficient and easy to implement, yet yields accurate results. As the proposed formulae are general in nature and applicable to wide range of materials with hexagonal nano-structures, the

present article can take a crucial role for characterizing the material properties in future nano-materials development.

## Acknowledgements

## References

[1] Balendhran, S., Walia, S., Nili, H., Sriram, S., and Bhaskaran, M. Elemental analogues of graphene: silicene, germanene, stanene, and phosphorene. *Small*, 11(6): 640–652, 2015.

[2] Xu, M., Liang, T., Shi, M., and Chen, H. Graphene–like two–dimensional materials. *Chemical Reviews*, 113(5):3766–3798, 2013.

[3] Das, S., Robinson, J. A., Dubey, M., Terrones, H., and Terrones, M. Beyond graphene: Progress in novel two-dimensional materials and van der waals solids. *Annual Review of Materials Research*, 45:1–27, 2015.

[4] Novoselov, K., Geim, A. K., Morozov, S., Jiang, D., Katsnelson, M., Grigorieva, I., Dubonos, S., and Firsov, A. Two-dimensional gas of massless dirac fermions in graphene. *Nature*, 438(7065):197–200, 2005.

[5] Geim, A. K. and Grigorieva, I. V. Van der waals heterostructures. *Nature*, 499(7459): 419–425, 2013.

[6] Zhang, Y. J., Yoshida, M., Suzuki, R., and Iwasa, Y. 2d crystals of transition metal dichalcogenide and their iontronic functionalities. *2D Materials*, 2(4):044004, 2015.

[7] Balandin, A. A., Ghosh, S., Bao, W., Calizo, I., Teweldebrhan, D., Miao, F., and Lau, C. N. Superior thermal conductivity of single-layer graphene. *Nano letters*, 8 (3):902–907, 2008.

[8] Zolyomi, V., Wallbank, J. R., and Fal'ko, V. I. Silicane and germanane: tight-binding and first-principles studies. *2D Materials*, 1(1):011005, 2014.

[9] Lorenz, T., Joswig, J.-O., and Seifert, G. Stretching and breaking of monolayer mos2 – an atomistic simulation. *2D Materials*, 1(1):011007, 2014.

[10] Liu, F., Ming, P., and Li, J. Ab initio calculation of ideal strength and phonon instability of graphene under tension. *Physical Review B*, 76(6):064120, 2007.

[11] Grantab, R., Shenoy, V. B., and Ruoff, R. S. Anomalous strength characteristics of tilt grain boundaries in graphene. *Science*, 330(6006):946–948, 2010.

[12] Chang, T. and Gao, H. Size-dependent elastic properties of a single-walled carbon nanotube via a molecular mechanics model. *Journal of the Mechanics and Physics of Solids*, 51(6):1059–1074, 2003.

[13] Scarpa, F., Adhikari, S., and Phani, A. S. Effective elastic mechanical properties of single layer graphene sheets. *Nanotechnology*, 20(6):065709, 2009.

[14] Shokrieh, M. M. and Rafiee, R. Prediction of young's modulus of graphene sheets and carbon nanotubes using nanoscale continuum mechanics approach. *Materials & Design*, 31:790–795, 2010.

[15] Boldrin, L., Scarpa, F., Chowdhury, R., and Adhikari, S. Effective mechanical properties of hexagonal boron nitride nanosheets. *Nanotechnology*, 22(50):505702, 2011.

[16] Le, M.-Q. Prediction of young's modulus of hexagonal monolayer sheets based on molecular mechanics. *International Journal of Mechanics and Materials in Design*, 11(1):15–24, 2015.

[17] Li, C. and Chou, T.-W. Static and dynamic properties of single-walled boron nitride nanotubes. *Journal of nanoscience and nanotechnology*, 6(1):54–60, 2006.

[18] Huang, C., Chen, C., Zhang, M., Lin, L., Ye, X., Lin, S., Antonietti, M., and Wang, X. Carbon-doped bn nanosheets for metal-free photoredox catalysis. *Nature communications*, 6, 7698, 2015.

[19] Vogt, P., Padova, P. D., Quaresima, C., Avila, J., Frantzeskakis, E., Asensio, M. C., Resta, A., Ealet, B., and Lay, G. L. Silicene: compelling experimental evidence for graphenelike two-dimensional silicon. *Physical review letters*, 108:155501, 2012.

[20] van den Broek, B., Houssa, M., Iordanidou, K., Pourtois, G., Afanasev, V. V., and Stesmans, A. Functional silicene and stanene nanoribbons compared to graphene: electronic structure and transport. *2D Materials*, 3(1):015001, 2016.

[21] Ni, Z., Liu, Q., Tang, K., Zheng, J., Zhou, J., Qin, R., Gao, Z., Yu, D., and Lu, J. Tunable bandgap in silicene and germanene. *Nano Letters*, 12(1):113–118, 2012.

[22] Liu, H., Neal, A. T., Zhu, Z., Luo, Z., Xu, X., TomÃ„ą̨nek, D., and Ye, P. D. Phosphorene: An unexplored 2d semiconductor with a high hole mobility. *ACS Nano*, 8 (4):4033–4041, 2014.

[23] Zhu, F., Chen, W., Xu, Y., Gao, C., Guan, D., Liu, C., Qian, D., Zhang, S., and Jia, J. Epitaxial growth of two-dimensional stanene. *Nature materials*, 14(10):1020–1025, 2015.

[24] Mannix, A. J., Zhou, X., Kiraly, B., Wood, J. D., Alducin, D., Myers, B. D., Liu, X., Fisher, B. L., Santiago, U., Guest, J. R., Yacaman, M. J., Ponce, A., Oganov, A. R., Hersam, M. C., and Guisinger, N. P. Synthesis of borophenes: Anisotropic, two-dimensional boron polymorphs. *Science*, 350(6267):1513–1516, 2015.

[25] Brunier, T. M., Drew, M. G. B., and Mitchell, P. C. H. Molecular mechanics studies of molybdenum disulphide catalysts parameterisation of molybdenum and sulphur. *Molecular Simulation*, 9(2):143–159, 1992.

[26] Zhao, W., Ghorannevis, Z., Chu, L., Toh, M., Kloc, C., Tan, P.-H., and Eda, G. Evolution of electronic structure in atomically thin sheets of ws2 and wse2. *ACS Nano*, 7(1):791–797, 2013.

[27] Coehoorn, R., Haas, C., Dijkstra, J., Flipse, C. J. F., de Groot, R. A., and Wold, A. Electronic structure of mose$_2$, mos$_2$, and wse$_2$. i. band-structure calculations and photoelectron spectroscopy. *Physical review B*, 35:6195–6202, 1987.

[28] Ruppert, C., Aslan, O. B., and Heinz, T. F. Optical properties and band gap of single- and few-layer mote2 crystals. *Nano Letters*, 14(11):6231–6236, 2014.

[29] Gelin, B. R. *Molecular Modeling of Polymer Structures and Properties*. Hanser Gardner Publications, 1994.

[30] Gibson, L. and Ashby, M. F. *Cellular Solids Structure and Properties*. Cambridge University Press, Cambridge, UK, 1999.

[31] Mukhopadhyay, T. and Adhikari, S. Equivalent in-plane elastic properties of irregular honeycombs: An analytical approach. *International Journal of Solids and Structures*, 91:169 − 184, 2016.

[32] Mukhopadhyay, T. and Adhikari, S. Effective in-plane elastic properties of auxetic honeycombs with spatial irregularity. *Mechanics of Materials*, 95:204 − 222, 2016.

[33] Mukhopadhyay, T. and Adhikari, S. Free vibration analysis of sandwich panels with randomly irregular honeycomb core. *Journal of Engineering Mechanics*, 10.1061/(ASCE)EM.1943-7889.0001153 , 06016008, 2016.

[34] Mukhopadhyay, T. and Adhikari, S. Stochastic mechanics of metamaterials. *Composite Structures*, 2016. doi: http://dx.doi.org/10.1016/j.compstruct.2016.11.080.

[35] Li, C. and Chou, T. W. A structural mechanics approach for the analysis of carbon nanotubes. *International Journal of Solids and Structures*, 40(10):2487 – 2499, 2003.

[36] Roark, R. J. and Young, W. C. *Formulas for Stress and Strain.* McGraw-Hill Book Company, 1976.

[37] Cornell, W. D., Cieplak, P., Bayly, C. I., Gould, I. R., Merz, K. M., Ferguson, D. M., Spellmeyer, D. C., Fox, T., Caldwell, J. W., and Kollman, P. A. A second generation force field for the simulation of proteins, nucleic acids, and organic molecules. *Journal of the American Chemical Society*, 117(19):5179–5197, 1995.

[38] Lee, C., Wei, X., Kysar, J. W., and Hone, J. Measurement of the elastic properties and intrinsic strength of monolayer graphene. *Science*, 321(5887):385–388, 2008.

[39] Demczyk, B., Wang, Y., Cumings, J., Hetman, M., Han, W., Zettl, A., and Ritchie, R. Direct mechanical measurement of the tensile strength and elastic modulus of multiwalled carbon nanotubes. *Materials Science and Engineering: A*, 334(1âĂŞ2): 173 – 178, 2002.

[40] Kudin, K. N., Scuseria, G. E., and Yakobson, B. I. C 2 f, bn, and c nanoshell elasticity from ab initio computations. *Physical Review B*, 64(23):235406, 2001.

[41] Lier, G. V., Alsenoy, C. V., Doren, V. V., and Geerlings, P. Ab initio study of the elastic properties of single-walled carbon nanotubes and graphene. *Chemical Physics Letters*, 326(1âĂŞ2):181 – 185, 2000.

[42] Sánchez-Portal, D., Artacho, E., Soler, J. M., Rubio, A., and Ordejón, P. *Ab initio* structural, elastic, and vibrational properties of carbon nanotubes. *Phys. Rev. B*, 59: 12678–12688, 1999.

[43] Jiang, J.-W., Wang, J.-S., and Li, B. Young's modulus of graphene: A molecular dynamics study. *Phys. Rev. B*, 80:113405, 2009.

[44] Zhao, H., Min, K., and Aluru, N. Size and chirality dependent elastic properties of

graphene nanoribbons under uniaxial tension. *Nano letters*, 9(8):3012–3015, 2009.

[45] Song, L., Ci, L., Lu, H., Sorokin, P. B., Jin, C., Ni, J., Kvashnin, A. G., Kvashnin, D. G., Lou, J., Yakobson, B. I., and Ajayan, P. M. Large scale growth and characterization of atomic hexagonal boron nitride layers. *Nano Letters*, 10(8):3209–3215, 2010.

[46] Peng, Q., Ji, W., and De, S. Mechanical properties of the hexagonal boron nitride monolayer: Ab initio study. *Computational Materials Science*, 56:11 – 17, 2012.

[47] Zhao, S. and Xue, J. Mechanical properties of hybrid graphene and hexagonal boron nitride sheets as revealed by molecular dynamic simulations. *Journal of Physics D: Applied Physics*, 46(13):135303, 2013.

[48] Le, M.-Q. Young's modulus prediction of hexagonal nanosheets and nanotubes based on dimensional analysis and atomistic simulations. *Meccanica*, 49(7):1709–1719, 2014.

[49] Jiang, L. and Guo, W. A molecular mechanics study on size-dependent elastic properties of single-walled boron nitride nanotubes. *Journal of the Mechanics and Physics of Solids*, 59(6):1204 – 1213, 2011.

[50] Oh, E. S. Elastic properties of various boron-nitride structures. *Metals and Materials International*, 17(1):21–27, 2011.

[51] Modarresi, M., Kakoee, A., Mogulkoc, Y., and Roknabadi, M. Effect of external strain on electronic structure of stanene. *Computational Materials Science*, 101:164 – 167, 2015.

[52] Castellanos-Gomez, A., Poot, M., Steele, G. A., van der Zant, H. S., Agraït, N., and Rubio-Bollinger, G. Elastic properties of freely suspended mos2 nanosheets. *Advanced Materials*, 24(6):772–775, 2012.

[53] Bertolazzi, S., Brivio, J., and Kis, A. Stretching and breaking of ultrathin MoS$_2$. *ACS Nano*, 5(12):9703–9709, 2011.

[54] Lorenz, T., Teich, D., Joswig, J.-O., and Seifert, G. Theoretical study of the mechanical behavior of individual TiS2 and MoS2 nanotubes. *The Journal of Physical Chemistry C*, 116(21):11714–11721, 2012.

[55] Scalise, E., Houssa, M., Pourtois, G., Afanas'ev, V., and Stesmans, A. Strain-induced semiconductor to metal transition in the two-dimensional honeycomb structure of

mos2. *Nano Research*, 5(1):43–48, 2012.

[56] Jiang, J.-W., Qi, Z., Park, H. S., and Rabczuk, T. Elastic bending modulus of single-layer molybdenum disulfide (mos2): finite thickness effect. *Nanotechnology*, 24(43): 435705, 2013.

[57] Blakslee, O., Proctor, D., Seldin, E., Spence, G., and Weng, T. Elastic constants of compression-annealed pyrolytic graphite. *Journal of Applied Physics*, 41(8):3373–3382, 1970.

[58] Sánchez-Portal, D., Artacho, E., Soler, J. M., Rubio, A., and Ordejón, P. Ab initio structural, elastic, and vibrational properties of carbon nanotubes. *Physical Review B*, 59(19):12678, 1999.

[59] Liu, F., Ming, P., and Li, J. *Ab initio* calculation of ideal strength and phonon instability of graphene under tension. *Phys. Rev. B*, 76:064120, 2007.

[60] Tu, Z.-c. and Ou-Yang, Z.-c. Single-walled and multiwalled carbon nanotubes viewed as elastic tubes with the effective young's moduli dependent on layer number. *Phys. Rev. B*, 65:233407, 2002.

[61] Jiang, J.-W., Wang, J.-S., and Li, B. Young's modulus of graphene: A molecular dynamics study. *Phys. Rev. B*, 80:113405, Sep 2009.

[62] Brenner, D. W. Empirical potential for hydrocarbons for use in simulating the chemical vapor deposition of diamond films. *Phys. Rev. B*, 42:9458–9471, 1990.

[63] Alzebdeh, K. Evaluation of the in-plane effective elastic moduli of single-layered graphene sheet. *International Journal of Mechanics and Materials in Design*, 8(3): 269–278, 2012. doi: 10.1007/s10999-012-9193-7.

[64] Alzebdeh, K. I. An atomistic-based continuum approach for calculation of elastic properties of single-layered graphene sheet. *Solid State Communications*, 177:25 – 28, 2014.

[65] Sakhaee-Pour, A. Elastic properties of single layered graphene sheet. *Solid State Communications*, 149:91–95, 2009.

[66] Akdim, B., Pachter, R., Duan, X., and Adams, W. W. Comparative theoretical study of single-wall carbon and boron-nitride nanotubes. *Phys. Rev. B*, 67:245404, 2003.

[67] Kudin, K. N., Scuseria, G. E., and Yakobson, B. I. $c_2F$, bn, and c nanoshell elasticity

from *ab initio* computations. *Phys. Rev. B*, 64:235406, 2001.

[68] Verma, V., Jindal, V. K., and Dharamvir, K. Elastic moduli of a boron nitride nanotube. *Nanotechnology*, 18(43):435711, 2007.

[69] Boldrin, L., Scarpa, F., Chowdhury, R., and Adhikari, S. Effective mechanical properties of hexagonal boron nitride nanosheets. *Nanotechnology*, 22(50):505702, 2011.

[70] Oh, E.-S. Elastic properties of boron-nitride nanotubes through the continuum lattice approach. *Materials Letters*, 64(7):859 − 862, 2010.

[71] Woo, S., Park, H. C., and Son, Y.-W. Poisson's ratio in layered two-dimensional crystals. *Phys. Rev. B*, 93:075420, 2016.

[72] Jiang, J.-W., Qi, Z., Park, H. S., and Rabczuk, T. Elastic bending modulus of single-layer molybdenum disulfide (mos 2 ): finite thickness effect. *Nanotechnology*, 24(43): 435705, 2013.

[73] Mayo, S. L., Olafson, B. D., and Goddard, W. A. Dreiding: a generic force field for molecular simulations. *The Journal of Physical Chemistry*, 94(26):8897–8909, 1990.

[74] Kudin, K. N., Scuseria, G. E., and Yakobson, B. I. $c_2F$, bn, and c nanoshell elasticity from *ab initio* computations. *Phys. Rev. B*, 64:235406, 2001.

[75] Oh, E. S. Elastic properties of boron-nitride nanotubes through the continuum lattice approach. *Materials Letters*, 64(7):859 − 862, 2010.

[76] Verma, V., Jindal, V. K., and Dharamvir, K. Elastic moduli of a boron nitride nanotube. *Nanotechnology*, 18(43):435711, 2007.

[77] Bosak, A., Serrano, J., Krisch, M., Watanabe, K., Taniguchi, T., and Kanda, H. Elasticity of hexagonal boron nitride: Inelastic x-ray scattering measurements. *Phys. Rev. B*, 73:041402, 2006.

[78] Wang, D., Chen, L., Wang, X., Cui, G., and Zhang, P. The effect of substrate and external strain on electronic structures of stanene film. *Phys. Chem. Chem. Phys.*, 17:26979–26987, 2015.

[79] Tang, P., Chen, P., Cao, W., Huang, H., Cahangirov, S., Xian, L., Xu, Y., Zhang, S.-C., Duan, W., and Rubio, A. Stable two-dimensional dumbbell stanene: A quantum spin hall insulator. *Phys. Rev. B*, 90:121408, 2014.

[80] van den Broek, B., Houssa, M., Scalise, E., Pourtois, G., Afanasev, V. V., and

Stesmans, A. Two-dimensional hexagonal tin: ab initio geometry, stability, electronic structure and functionalization. *2D Materials*, 1(2):021004, 2014.

[81] Radisavljevic, B., Radenovic, A., Brivio, J., Giacometti, i. V., and Kis, A. Single-layer mos2 transistors. *Nature nanotechnology*, 6(3):147–150, 2011.

[82] Bronsema, K., De Boer, J., and Jellinek, F. On the structure of molybdenum dise-lenide and disulfide. *Zeitschrift für anorganische und allgemeine Chemie*, 540(9-10): 15–17, 1986.

[83] Schönfeld, B., Huang, J., and Moss, S. Anisotropic mean-square displacements (msd) in single-crystals of 2h-and 3r-mos2. *Acta Crystallographica Section B: Structural Science*, 39(4):404–407, 1983.

[84] Wieting, T. and Verble, J. Infrared and raman studies of long-wavelength optical phonons in hexagonal mos2. *Physical Review B*, 3(12):4286, 1971.

[85] Ma, Z. and Dai, S. Ab initio studies on the electronic structure of the complexes containing moâĂŤs bond using relativistic effective core potentials. *Acta Chimica Sinica English Edition*, 7(3):201–208, 1989.

[86] Castellanos-Gomez, A., van Leeuwen, R., Buscema, M., van der Zant, H. S., Steele, G. A., and Venstra, W. J. Single-layer mos2 mechanical resonators. *Advanced Materials*, 25(46):6719–6723, 2013.

[87] Li, T. Ideal strength and phonon instability in single-layer mos 2. *Physical Review B*, 85(23):235407, 2012.